Analytical Methods

PAPER

View Article Online
View Journal | View Issue



Cite this: *Anal. Methods*, 2018, **10**, 5341

# A $MnO_2$ nanosheets–*o*-phenylenediamine oxidative system for the sensitive fluorescence determination of alkaline phosphatase activity†

Xionghong Tan,[abc] Zheng Li,[d] Yanlin Du,[abc] Aixian Zheng,[c] Yongyi Zeng,[c] Xiaolong Zhang,*[c] Xiaolong Liu*[bc] and Niancai Peng*[d]

Alkaline phosphatase (ALP) plays a crucial role in the regulation of intracellular processes and acts as an important biomarker for diagnosis of diverse diseases. Herein, we report a selective, sensitive and convenient sensing assay for detecting ALP based on a $MnO_2$ nanosheets–*o*-phenylenediamine (OPDA) oxidative system. In this system, the $MnO_2$ nanosheets could effectively oxidize OPDA to produce fluorescent OPDAox for fluorescence detection, while the incubation of $MnO_2$ nanosheets with ascorbic acid (AA) would first lead to the reduction of the $MnO_2$ nanosheets and then inhibit the formation of fluorescent OPDAox. Based on this principle, a sensitive and rapid method for fluorescence sensing of AA with a good linear relationship from 0.1 to 50 μM ($R^2$ = 0.9962) was achieved. ALP can enzymatically hydrolyze 2-phospho-L-ascorbic acid (AAP) to produce AA, which could reduce the $MnO_2$ nanosheets and inhibit the oxidation of OPDA to fluorescent OPDAox. Then, the $MnO_2$ nanosheets–OPDA sensing system was applied to detect ALP. This fluorescence sensing system could detect ALP activity selectively, sensitively and conveniently with a good linear relationship from 0.1 to 200 U $L^{-1}$ ($R^2$ = 0.9946); meanwhile, this system was also applied to detect ALP in human serum samples. Taken together, the proposed $MnO_2$–OPDA oxidative system shows promising potential in biomedical applications.

Received 19th September 2018
Accepted 25th October 2018

DOI: 10.1039/c8ay02061b

rsc.li/methods



## Introduction

Alkaline phosphatase (ALP) is an important and universal hydrolase enzyme for catalysis of the dephosphorylation process on a wide variety of phosphorylated substrates, including proteins, nucleic acids, and small molecules.[1] The dephosphorylation process of ALP plays a vital role in signal transduction and regulation of protein activity. The abnormal dephosphorylation of these substrates may give rise to an imbalance of organ metabolism and development of several diseases, including bone diseases, hepatitis, diabetes, prostate cancer, liver cancer and renal cell carcinoma.[2–7] The level of serum ALP, to a certain extent, as a key indicator and biomarker for estimation of the dephosphorylation rate of the phosphorylated substances described above, represents the state of the human body.[8,9] Therefore, the alteration of the ALP level and activity is commonly used as a clarifying and predicting indicator for many diseases. To date, various methods have been developed for detecting and quantifying the ALP activity in diagnostic tests and biochemical analysis, such as chromatography,[10] surface enhanced Raman scattering,[11,12] UV-vis absorption,[13] electrochemical analysis[14–17] and fluorescence.[18–20] It is well known that fluorescence-based methods are worthy of further development due to their simplicity, rapid implementation and high sensitivity as well as real-time detection. So far, a variety of fluorescent probes have been developed, including semiconductor quantum dots (QDs),[1,21] organic dyes,[22] fluorescent noble metal nanoparticles,[23] coordination polymers,[24] *etc.* However, follow-up studies found that these materials still exhibit some drawbacks, such as toxicity for QDs, high costs for noble metal nanoprobes, and complex synthesis processes for organic dyes and coordination polymers. Thus, it is still highly desirable to develop new methods with non-toxicity, simpler synthesis, cost-effectiveness and simple operability for sensing ALP activity.[25]

Recently, manganese dioxide ($MnO_2$) nanosheets, as a new emerging nano-quencher first reported by Liu's group,[26] have attracted great research interest due to their striking advantages, including good biocompatibility, low cost, large surface area and rigidity, good redox properties and excellent absorption

[a]*College of Life Science, Fujian Agriculture and Forestry University, Fuzhou, Fujian 350002, P. R. China*

[b]*Fujian Institute of Research on the Structure of Matter, Chinese Academy of Sciences, Fuzhou, Fujian 350002, P. R. China. E-mail: xiaoloong.liu@gmail.com*

[c]*The United Innovation of Mengchao Hepatobiliary Technology Key Laboratory of Fujian Province, Mengchao Hepatobiliary Hospital of Fujian Medical University, Fuzhou 350025, PR China. E-mail: xiaolongdo@gmail.com*

[d]*State Key Laboratory for Manufacturing System Engineering, School of Mechanical Engineering, Xi'an Jiaotong University, Xi'an 710049, P. R. China. E-mail: pnc@mail.xjtu.edu.cn*

† Electronic supplementary information (ESI) available: Fig. S1–S7 and Table S1. See DOI: 10.1039/c8ay02061b

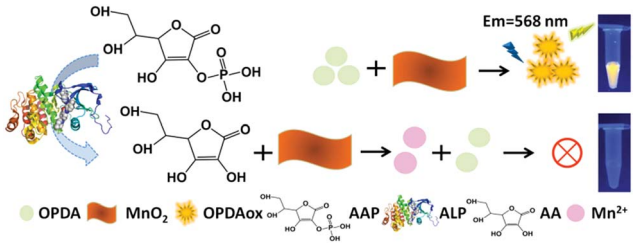


Fig. 1 Schematic illustration for detecting alkaline phosphatase *via* the $MnO_2$–OPDA sensing system.

capability.[26–28] As a consequence, $MnO_2$ nanosheets as an super quencher and/or nanocarrier have been widely used in various of bionanomedicine fields, such as tumor cell imaging,[29] biosensing systems for biomarkers,[30,31] and drug delivery.[32] In addition, $MnO_2$ nanosheets were also used as mimetic enzymes for enzyme-linked immunosorbent assay,[33] colorimetric assay for glutathione (GSH),[28] fluorescence detection for ALP activity,[34] and electrochemical determination for GSH.[35] Therefore, $MnO_2$ nanosheets attract great attention for developing novel biosensing platforms.

Herein, we report a selective, sensitive, low-cost and convenient method for fluorescence detection of ALP activity using a $MnO_2$ nanosheets–OPDA sensing system (Fig. 1). The effective oxidant $MnO_2$ nanosheets could effectively oxidize OPDA to fluorescent 2,3-diaminophenazine (OPDAox); however, upon pre-incubation with AA, the $MnO_2$ nanosheets would be reduced to $Mn^{2+}$ and inhibit the formation of fluorescent OPDAox. Thus, the redox reaction between $MnO_2$ nanosheets and AA could be used for AA detection. Meanwhile, ALP could enzymatically hydrolyze 2-phospho-L-ascorbic acid (AAP) to yield AA, which then triggered the reduction of $MnO_2$ nanosheets and inhibited the production of fluorescent OPDAox.[30] Based on the above reaction process, the ALP activity could be determined selectively, sensitively and conveniently. Moreover, this sensing system was used to probe ALP in human serum samples, and it demonstrated great potential for application in clinical bioanalysis and screening potential ALP inhibitors.

# Experimental

## Materials

Glycine (Gly), glucose oxidase (GOx), 3-morpholinopropanesulfonic acid (MOPS), alkaline phosphatase (ALP) and *o*-phenylenediamine (OPDA) were purchased from Shanghai Sangon Biothenology Co., Ltd. (China). $KMnO_4$ and L-cysteine (L-Cys) were obtained from Sinopharm Chemical Reagent Co., Ltd. (China). L-Leucine was purchased from Solarbio Co., Ltd. (China). *N*-Ethylmaleimide (NEM), ascorbic acid (AA), GSH (reduced form) and bovine serum albumin (BSA) were purchased from Sigma-Aldrich. Other reagents of analytical reagent grade were purchased from Sinopharm Chemical Reagent Co., Ltd. (China), and were used as received. Human serum samples were provided by Mengchao Hepatobiliary Hospital of Fujian Medical University. The study was approved by the Medical Ethics Committee of Mengchao Hepatobiliary Hospital of Fujian Medical University in accordance with the relevant laws and institutional guidelines of the Ministry of Health of P. R. China, namely the ethical principles for medical research involving human subjects, and written consent was received from all participants in this study. Ultrapure water (18.2 MΩ cm at room temperature) was prepared from a Millipore water purification system and used in all the experiments.

## Instruments

Fluorescence spectra measurements were performed on an Agilent Cary Eclipse fluorescence spectrophotometer. Ultraviolet-visible light (UV-vis) absorption spectra were recorded in 1 cm-path-length quartz cuvettes on a microplate reader (Spectra 206 Max M5, Molecular Devices). Transmission electron microscopy (TEM) images were recorded on a field emission high resolution 2100F TEM (JEOL, Japan) with an acceleration voltage of 200 kV.

## Preparation of $MnO_2$ nanosheets

The $MnO_2$ nanosheets were prepared according to reported methods.[36,37] First, a mixture of $KMnO_4$ (0.1 mmol) and MOPS buffer (1 mmol) in 10 mL ultrapure water was prepared. Then the mixture was sonicated for 30 min. The brown solution was centrifuged at 10 000 rpm for 5 min. Thereafter, the excess potassium and free manganese ions were removed by washing with ultrapure water three times. Finally, the solution of $MnO_2$ nanosheets was diluted to 1 mg $mL^{-1}$ with ultrapure water and dispersed by ultrasonic treatment.

## Detection of AA based on the $MnO_2$ nanosheets–OPDA sensing system

For the typical fluorescence sensing of AA, 2.5 μL of $MnO_2$ nanosheets (1 mg $mL^{-1}$) were firstly incubated with 200 μL of different concentrations of AA dissolved in PBS buffer (0.2 M, pH = 7.4). After reaction for 10 min, 3 μL of OPDA solution (5 mM) was introduced into the mixtures and then reacted at 50 °C for 10 min. Finally, the UV-vis absorption spectrum and fluorescence emission spectra with excitation at 420 nm were measured.

## Detection of ALP activity based on the $MnO_2$ nanosheets–OPDA sensing system

For fluorescence detection of ALP activity, 50 μL of AAP (20 mM) dissolved in PBS buffer (0.2 M, pH = 7.4) and 100 μL of different concentrations of ALP dissolved in PBS buffer (0.2 M, pH = 8.0) were incubated at 37 °C for 30 min firstly. Next, 2.5 μL of $MnO_2$ nanosheets (1 mg $mL^{-1}$) and 50 μL of PBS buffer (0.2 M, pH = 7.4) were added into the above mixtures and incubated for another 10 min. After that, 3 μL of OPDA solution (5 mM) was added into the mixtures and then reacted at 50 °C for 10 min. Finally, the UV-vis absorption spectra were recorded from 300 nm to 550 nm and fluorescence emission spectra were recorded from 500 nm to 700 nm with excitation at 420 nm. For the detection of ALP activity in human serum samples, the samples were diluted 25 times with PBS buffer (0.2 M, pH = 7.4),

 

and then 0.2 mM NEM was added to block the biothiols. After incubation at 37 °C for 30 min, different concentrations of ALP were spiked with the pre-treated human serum solution. Finally, 100 μL of serum samples with added ALP were used as the final samples. Then, the samples were measured as described above.

## Results and discussion

### Development of the $MnO_2$ nanosheets–OPDA oxidative system

In the present study, the $MnO_2$ nanosheets served as an effective oxidant for OPDA and recognizer for AA, and they were prepared by reducing $KMnO_4$ in MOPS buffer according to previous reports.[36,37] As shown in Fig. 2A, the prepared $MnO_2$ nanosheets show a wide absorbance spectrum from 200 to 700 nm, which is an optical characteristic of $MnO_2$ nanomaterials.[31] The change of absorbance spectrum and color of $KMnO_4$ solution also indicated the reduction of $KMnO_4$. The TEM image shows the typical nanosheet morphology of $MnO_2$ (Fig. 2B), which matched well with that of the reported $MnO_2$ nanosheets.[36] Therefore, the $MnO_2$ nanosheets were successfully prepared. Next, we tested the performance of the $MnO_2$ nanosheets–OPDA based oxidative system. OPDA, used as a fluorescent detection probe, was colorless and nonfluorescent before oxidation, and it turned light yellow and exhibited bright orange fluorescence after being oxidized by $MnO_2$ nanosheets. As shown in Fig. 2C and D, compared with the OPDA solution or $MnO_2$ nanosheets alone, the oxidized product OPDAox showed a very intense maximum absorption band around 420 nm and a fluorescence emission peak at around 568 nm. The corresponding photographs under daylight and UV light in the figure insets also indicated the synthesized fluorescent OPDAox.

To obtain a good fluorescence detection signal, we examined the reaction conditions, including the pH, reaction time, temperature and dose of $MnO_2$ nanosheets. As shown in the Fig. S1–S4,† the optimal reaction conditions were selected as follows: pH 7.4, 50 °C and 10 min. At the above conditions, the fluorescence intensity of OPDAox at 568 nm was dependent on the concentration of $MnO_2$ nanosheets in the range of 0–12.5 μg $mL^{-1}$. So, 12.5 μg $mL^{-1}$ $MnO_2$ nanosheets were used for detection. Because of the effective oxidative activity of $MnO_2$ nanosheets, the fluorescence intensity of OPDAox could be successfully regulated, suggesting the possibility of using this $MnO_2$–OPDA oxidative system for detecting reducing substances.

### AA sensing based on the $MnO_2$ nanosheets–OPDA oxidative system

To explore the application of the $MnO_2$ nanosheets–OPDA oxidative system, AA was chosen as a reductant to chemically reduce and consume $MnO_2$ nanosheets, which thereby inhibit the formation of fluorescent OPDAox. We first investigated the optimal reaction time and 5 min was chosen as the appropriate incubation time for AA sensing according to the result from Fig. S5.† As presented in Fig. 3A and B, the absorption and fluorescence of OPDAox were found to be inhibited for 5 min. The corresponding photograph (inset in Fig. 3B) also showed that the production of bright orange fluorescent OPDAox was inhibited upon addition of AA. The UV-vis absorption spectra and the corresponding photograph of $MnO_2$ nanosheets before and after AA treatment are shown in Fig. S6.† The characteristic absorption band of $MnO_2$ nanosheets disappeared after incubation with AA, further suggesting the decomposition of $MnO_2$ nanosheets to $Mn^{2+}$ by AA. These results imply the possibility of

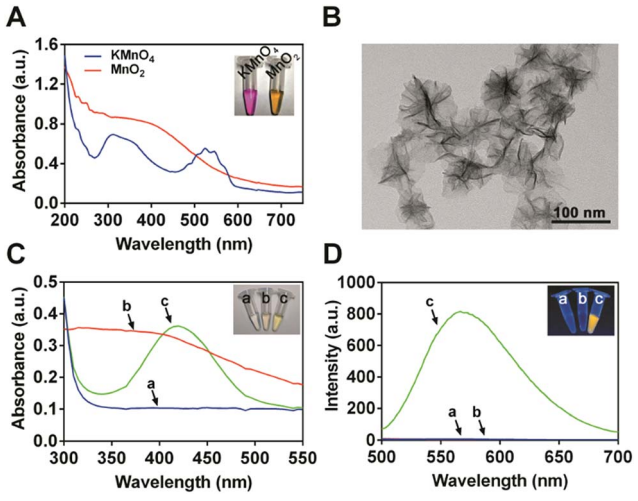


Fig. 2 (A) The UV-vis absorption of $KMnO_4$ (1 mM) and $MnO_2$ (25 μg $mL^{-1}$), respectively. The insets are photographs of the corresponding solutions; (B) TEM image of the as-prepared $MnO_2$. Scale bar: 100 nm; (C) UV-vis absorption spectra and (D) fluorescence emission spectra of (a) OPDA solution, (b) $MnO_2$ nanosheet solution and (c) $MnO_2$ nanosheets + OPDA solution. The insets show the photographs of the corresponding solutions under visible light (C) and 365 nm UV light (D). Concentrations: OPDA, 75 μM; $MnO_2$, 12.5 μg $mL^{-1}$.

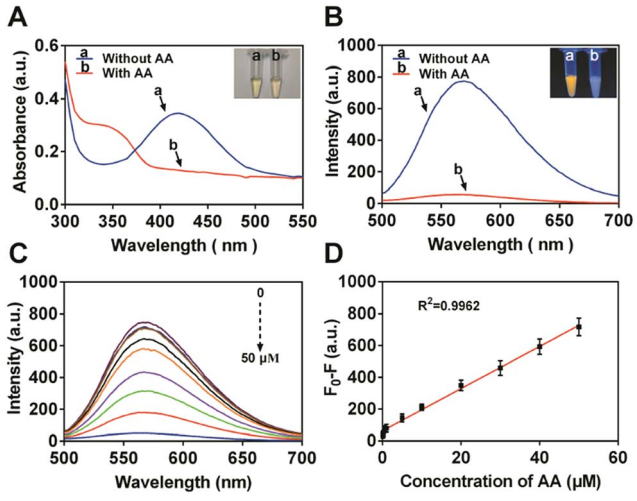


Fig. 3 (A) UV-vis absorption spectrum and (B) fluorescence emission spectrum in the absence of AA (a) and presence of 50 μM AA (b). The insets show the photographs of the corresponding solutions under visible light (A) and 365 nm UV light (B). (C) Fluorescence emission spectrum *versus* different concentrations of AA. (D) The linear relationship between fluorescence intensity change values ($F_0 - F$) and the concentration of AA ranging from 0.1 to 50 μM. $F_0$ and $F$ denote fluorescence intensity in the absence and presence of AA, respectively.

using this $MnO_2$–OPDA oxidative system for sensing AA. Next, various concentrations of AA were measured using this sensing system.

As shown in Fig. 3C, the fluorescence intensity of OPDAox decreased with increasing concentration of AA. The calibration curve for AA sensing under the standard conditions was determined as $(F_0 - F) = 13.30[AA] + 62.42$ with a correlation coefficient of 0.9962 ($n = 3$) over the range of 0.1 to 50 μM (Fig. 3D). Thus, the $MnO_2$ nanosheets–OPDA system could be utilized as a potential and optional way for detecting AA and its related biomolecules.

### ALP detection based on the $MnO_2$ nanosheets–OPDA oxidative system

ALP can enzymatically hydrolyze AAP to AA, which could be used for ALP activity detection by the AA response sensing platform.[30] Therefore, to verify the possibility of detecting ALP with the assistance of AAP using this proposed system, we first studied the effect of AAP on the fluorescence of OPDAox. As shown in Fig. S7,† AAP or ALP alone did not induce any substantial fluorescence decrease of OPDAox, while the coexistence of AAP and ALP could lead to an obvious fluorescence decrease of OPDAox due to the generation of AA. This result indicated that AAP or ALP alone had little effect on the fluorescence of OPDAox and ALP could hydrolyze AAP to AA, which then triggered the decomposition of $MnO_2$ nanosheets. So, the incubation of ALP with AAP would first lead to the inhibition of the formation of OPDAox and then significantly reduce the absorption and fluorescence of OPDAox (Fig. 4A and B). These results implied the possibility of ALP activity detection using the $MnO_2$ nanosheets–OPDA system. Then we determined the relationship between the fluorescence change of the system and the concentration of ALP. The fluorescence of OPDAox was found to progressively decrease with the increase of ALP concentration (Fig. 4C). The equation was determined to be $(F_0 - F) = 1.44[ALP] + 46.0$ with a good linear relationship $R^2 = 0.9946$ ($n = 3$) over the range of 0.1 to 200 U $L^{-1}$. Also, by comparing with different methods for the detection of ALP activity in Table S1,† we give evidence to show that the developed sensing method is comparable to previously reported methods, and could be used for practical ALP assay which covered the normal level of ALP in human serum (about 40 to 190 U $L^{-1}$).[38]

To further evaluate the specificity of the $MnO_2$ nanosheets–OPDA sensing system toward ALP, the selectivity of the system for various potential interferents, including some metal ions, amino acids and proteins, was tested. The results showed that other interferents, except GSH, were unable to bring about a significant alteration of fluorescence of the system, and only the target ALP could cause a remarkable effect on the sensing system (Fig. 5). In line with the principle of the sensing system described above, the potential reducing species GSH can also inhibit the fluorescence of the sensing system for detecting ALP. However, the inhibition effect of GSH could be reversed in the presence of NEM, which can specifically block the thiols of GSH. These results demonstrated that the developed sensing platform showed excellent specificity and selectivity for detecting ALP and this system is a promising and optional tool for detection of ALP in practical assay.

### Sensing ALP activity in human serum

To evaluate the practical applications of the $MnO_2$ nanosheets–OPDA sensing system, the detection of ALP activity in human serum samples was performed. In order to avoid the potential reductive interferents in serum (GSH and L-Cys), the serum samples were centrifuged at 12 000 rpm for 10 min and then, to the resulting supernatant, 0.2 mM NEM as the specific thiol-blocking compound was added.[31,39] As shown in Table 1, recoveries of 92.92–109.44% were obtained, with relative standard deviations (RSD) ranging from 0.72% to 2.21%. The results indicated that the $MnO_2$ nanosheets–OPDA sensing system can be utilized to detect and analyze the activity of ALP in real biological samples.

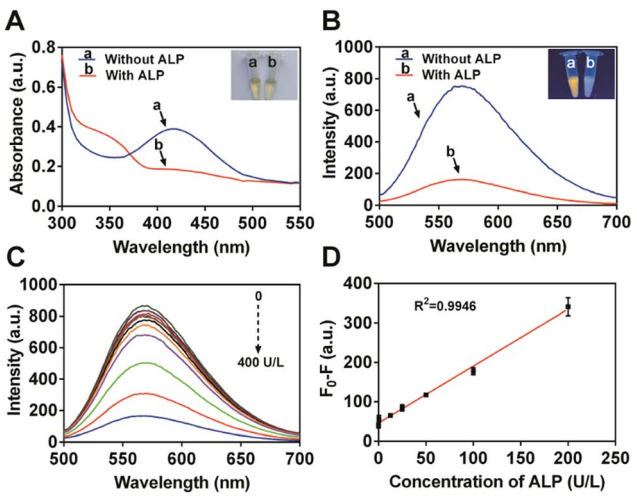


Fig. 4 (A) UV-vis absorption spectrum and (B) fluorescence emission spectrum in the absence of ALP (a) and presence of 400 U $L^{-1}$ ALP (b). The insets show the photographs of the corresponding solutions under visible light (A) and 365 nm UV light (B). (C) Fluorescence emission spectrum *versus* different concentrations of ALP. (D) The linear relationship between the fluorescence intensity change values $(F_0 - F)$ and the concentration of ALP ranging from 0.1 to 200 U $L^{-1}$. $F_0$ and $F$ denote fluorescence intensity in the absence and presence of ALP, respectively.

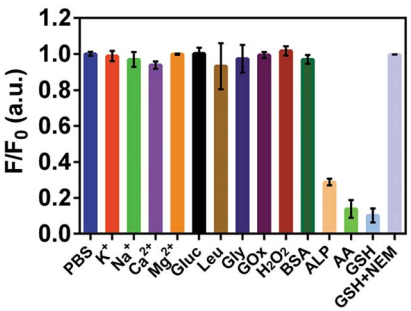


Fig. 5 Selectivity of ALP over potential interferents. PBS, 0.2 M; KCl, NaCl, $CaCl_2$, $MgCl_2$, and glucose, 1 mM; Leu and Gly, 40 μM; GOx, 0.01 mg $mL^{-1}$; $H_2O_2$, 10 μM; BSA, 1 mg $mL^{-1}$; ALP, 400 $UL^{-1}$; AA and GSH, 50 μM; NEM, 200 μM.

Table 1 Determination of ALP in human serum samples

| Sample no. | 1 | 2 | 3 | 4 |
|---|---|---|---|---|
| Amount of ALP added (U $L^{-1}$) | 20 | 30 | 50 | 70 |
| Amount of ALP detected (U $L^{-1}$) | 18.58 | 29.10 | 50.12 | 76.61 |
| Recovery | 92.92 | 97.01 | 100.24 | 109.44 |
| RSD ($n = 3$, %) | 0.72 | 2.21 | 1.14 | 0.98 |

## Conclusions

In summary, we demonstrated a selective, sensitive and convenient sensing assay for ALP sensing based on a $MnO_2$ nanosheets–OPDA system. In this assay, OPDA could be oxidized to fluorescent OPDAox with the oxidation of $MnO_2$ nanosheet solution. However, the $MnO_2$ nanosheets can be decomposed by AA, and reduced to $Mn^{2+}$; thereafter the generation of fluorescent OPDAox is inhibited. ALP is capable of enzymatically hydrolysing AAP to produce AA, and thus with the assistance of AAP, the activity of ALP could be sensitively and selectively detected using the $MnO_2$ nanosheets–OPDA sensing system. Therefore, we expect that this system can be used to detect and analyze other biomolecules related with $MnO_2$ response, and expand its application in clinical diagnosis and biomedical research.

## Conflicts of interest

There are no conflicts to declare.

## Acknowledgements

This work was supported by the National Natural Science Foundation of China (Grant No. 21605021, 21705022, 61675164, and 61827827), Joint Funds for the Innovation of Science and Technology of Fujian province (Grant No. 2016Y9060 and 2017Y9115), the Natural Science Foundation of Fujian Province of China (Grant No. 2016J05206), the Young and Middle-aged Talent Training Project of Fujian Provincial Health and Family Planning Commission (Grant No. 2018-ZQN-75) and the Medical Innovation grant of Fujian province (Grant No. 2018-CX-49).

## Notes and references

1 S. Liu, X. Wang, S. Pang, W. Na, X. Yan and X. Su, *Anal. Chim. Acta*, 2014, **827**, 103–110.
2 M. M. Couttenye, P. C. D'Haese, V. O. V. Hoof, E. Lemoniatou, W. Goodman, G. A. Verpooten and M. E. D. Broe, *Nephrology, dialysis, transplantation : official publication of the European Dialysis and Transplant Association*, European Renal Association, 1996, vol. 11, pp. 1065–1072.
3 K. Kaliannan, S. R. Hamarneh, K. P. Economopoulos, A. S. Nasrin, O. Moaven, P. Patel, N. S. Malo, M. Ray, S. M. Abtahi and N. Muhammad, *Proc. Natl. Acad. Sci. U. S. A.*, 2013, **110**, 7003–7008.
4 D. W. Moss, *Clin. Biochem.*, 1987, **20**, 225–230.
5 P. Colombatto, A. Randone, G. Civitico, G. J. Monti, L. Dolci, N. Medaina, F. Oliveri, G. Verme, G. Marchiaro and R. Pagni, *J. Viral Hepatitis*, 2010, **3**, 301–306.
6 A. Fatemeh, H. Hossein, I. Maznah, A. J. Domb, O. A. Rahman, C. P. Pei, P. D. Hong, D. S. Yu and F. Ira-Yudovin, *Int. J. Nanomed.*, 2012, **7**, 4159–4168.
7 K. B. Whitaker, D. Eckland, H. J. Hodgson, S. Saverymuttu, G. Williams and D. W. Moss, *Clin. Chem.*, 1982, **28**, 374–377.
8 M. W. Saif, D. Alexander and C. M. Wicox, *J. Appl. Res.*, 2005, **5**, 88–95.
9 A. Deeb and A. Elfatih, *J. Clin. Res. Pediatr. Endocrinol.*, 2018, **10**, 19–24.
10 P. Magnusson, O. Löfman and L. Larsson, *J. Chromatogr. B: Biomed. Sci. Appl.*, 1992, **576**, 79–86.
11 Y. Zeng, J. Q. Ren, S. K. Wang, J. M. Mai, B. Qu, Y. Zhang, A. G. Shen and J. M. Hu, *ACS Appl. Mater. Interfaces*, 2017, **9**, 29547–29553.
12 J. Dong, Y. Li, M. Y. Zhang, L. Zhang, T. Y. Yan and W. P. Qian, *Anal. Methods*, 2014, **6**, 9168–9172.
13 Z. Zhang, Z. Chen, F. Cheng, Y. Zhang and L. Chen, *Analyst*, 2016, **141**, 2955–2961.
14 N. M. Hemed, A. Convertino and Y. Shacham-Diamand, *Sens. Actuators, B*, 2018, **259**, 809–815.
15 W. Sun and K. Jiao, *Bull. Chem. Soc. Ethiop.*, 2005, **19**, 163–173.
16 P. Fanjul-Bolado, D. Hernández-Santos, M. B. González-García and A. Costa-García, *Anal. Chem.*, 2007, **79**, 5272–5277.
17 J. Peng, X. X. Han, Q. C. Zhang, H. Q. Yao and Z. N. Gao, *Anal. Chim. Acta*, 2015, **878**, 87–94.
18 C. X. Chen, J. H. Zhao, Y. Z. Lu, S. Jian and X. R. Yang, *Anal. Chem.*, 2018, **90**, 3505–3511.
19 J. Y. Du, L. Q. Xiong, C. B. Ma, H. S. Liu, J. Wang and K. M. Wang, *Anal. Methods*, 2016, **8**, 5095–5100.
20 R. M. Kong, T. Fu, N. N. Sun, F. L. Qu, S. F. Zhang and X. B. Zhang, *Biosens. Bioelectron.*, 2013, **50**, 351–355.
21 R. Freeman, T. Finder, R. Gill and I. Willner, *Nano Lett.*, 2010, **10**, 2192–2196.
22 W. J. Zhang, H. X. Yang, N. Li and N. Zhao, *RSC Adv.*, 2018, **8**, 14995–15000.
23 L. Zhang, J. Zhao, M. Duan, H. Zhang, J. Jiang and R. Yu, *Anal. Chem.*, 2013, **85**, 3797–3801.
24 J. Deng, P. Yu, Y. Wang and L. Mao, *Anal. Chem.*, 2015, **87**, 3080–3086.
25 S. G. Liu, L. Han, N. Li, N. Xiao, Y. J. Ju, N. B. Li and H. Q. Luo, *J. Mater. Chem. A*, 2018, **6**, 2843–2850.
26 R. Deng, X. Xie, M. Vendrell, Y. T. Chang and X. Liu, *J. Am. Chem. Soc.*, 2011, **133**, 20168–20171.
27 D. Fan, C. Shang, W. Gu, E. Wang and S. Dong, *ACS Appl. Mater. Interfaces*, 2017, **9**, 25870–25877.
28 J. Liu, L. Meng, Z. Fei, P. J. Dyson, X. Jing and X. Liu, *Biosens. Bioelectron.*, 2017, **90**, 69–74.
29 Z. Zhao, H. Fan, G. Zhou, H. Bai, H. Liang, R. Wang, X. Zhang and W. Tan, *J. Am. Chem. Soc.*, 2014, **136**, 11220–11223.
30 T. Xiao, J. Sun, J. Zhao, S. Wang, G. Liu and X. Yang, *ACS Appl. Mater. Interfaces*, 2018, **10**, 6560–6569.
31 C. P. Yao, W. Jing, A. X. Zheng, L. J. Wu, X. L. Zhang and X. L. Liu, *Sens. Actuators, B*, 2017, **252**, 30–36.

32 Y. Chen, D. L. Ye, M. Y. Wu, H. R. Chen, L. L. Zhang, J. L. Shi and L. Z. Wang, *Adv. Mater.*, 2015, **26**, 7018.
33 Y. Wan, P. Qi, D. Zhang, J. Wu and Y. Wang, *Biosens. Bioelectron.*, 2012, **33**, 69–74.
34 F. Qu, H. Pei, R. Kong, S. Zhu and X. Lian, *Talanta*, 2017, **165**, 136–142.
35 Q. Tan, R. Zhang, R. Kong, W. Kong, W. Zhao and F. Qu, *Microchim. Acta*, 2018, **185**, 44.
36 Z. Z. Dong, L. Lu, C. N. Ko, C. Yang, S. Li, M. Y. Lee, C. H. Leung and D. L. Ma, *Nanoscale*, 2017, **9**, 4677–4682.
37 X. L. Zhang, C. Zheng, S. S. Guo, J. Li, H. H. Yang and G. Chen, *Anal. Chem.*, 2014, **86**, 3426–3434.
38 G. Li, H. Fu, X. Chen, P. Gong, G. Chen, L. Xia, H. Wang, J. M. You and Y. Wu, *Anal. Chem.*, 2016, **88**, 2720–2726.
39 J. Yuan, Y. Cen, X. J. Kong, S. Wu, C. L. Liu, R. Q. Yu and X. Chu, *ACS Appl. Mater. Interfaces*, 2015, **7**, 10548–10555.